

- [10] H. M. Greenhouse, "Design of planar rectangular microelectronic inductors," *IEEE Trans. Parts, Hybrids, Packag.*, vol. PHP-10, pp. 101–109, June 1974.
- [11] Y.-C. Ho, K. Kim, B. Floyd, C. Wann, Y. Taur, I. Lagnado, and K. O, "4-GHz and 13-GHz tuned amplifiers implemented in a 0.1- μ m CMOS technology on SOI, SOS and bulk substrates," *IEEE J. Solid-State Circuits*, vol. 33, pp. 2066–2073, Dec. 1998.
- [12] K. K. O, "Estimation methods for quality factors of inductors fabricated in silicon integrated circuit process technologies," *IEEE J. Solid-State Circuits*, vol. 33, pp. 1249–1252, Aug. 1998.
- [13] B. A. Floyd, L. Shi, Y. Taur, I. Lagnado, and K. K. O, "SOI and bulk CMOS frequency dividers operating above 15 GHz," *Electron. Lett.*, vol. 37, no. 10, pp. 617–618, May 2001.
- [14] C. P. Yue and S. S. Wong, "On-chip spiral inductors with patterned ground shields for Si-based RF IC's," *IEEE J. Solid-State Circuits*, vol. 33, pp. 743–752, May 1998.
- [15] B. A. Floyd, C.-M. Hung, and K. K. O, "A 15-GHz wireless interconnect implemented in a 0.18- μ m CMOS technology using integrated transmitters, receivers and antennas," in *IEEE Very Large Scale Integration Circuits Tech. Symp. Dig.*, June 2001, pp. 155–158.
- [16] B. A. Floyd, "A CMOS wireless interconnect system for multigigahertz clock distribution," Ph.D. dissertation, Dept. Elect. Comput. Eng., Univ. Florida, Gainesville, FL, 2001.

Effect of Conductive Perturber Diameter on Nonresonant Measurement of Interaction Impedance for Helical Slow-Wave Structures

Sun-Shin Jung, Andrei V. Soukhov, and Gun-Sik Park

Abstract—The measurement accuracy of the interaction impedance for a helical slow-wave structure (SWS) using the nonresonant perturbation method has been studied using conductive wire perturbers with different diameters. Data obtained by the measurement were compared with a rigorous numerical analysis. It is shown that the measured values of the interaction impedance for the helical SWS converge to those obtained by using a three-dimensional finite-element computational method when the diameter of the perturber is reduced to less than 10% of the helix diameter.

Index Terms—Helical slow-wave structure, interaction impedance, nonresonant perturbation measurement, traveling-wave tube.

I. INTRODUCTION

An accurate estimation of interaction impedance, which is correlated with gain and efficiency of a device such as a traveling-wave tube (TWT), is an important step for the design of the device. On-axis interaction impedance was defined by Pierce [1] as

$$K = \frac{E_z^2}{2\beta_0^2 P} \quad (1)$$

Manuscript received May 11, 2001. This work was supported in part by the Ministry of Defense of Korea under a contract from KMW Inc., and in part by the Ministry of Science and Technology of Korea under the National Research Laboratory Program.

S.-S. Jung was with the Vacuum Electrophysics Laboratory, School of Physics, Seoul National University, Seoul 151-742, Korea. He is now with the Applied Electrophysics Group, Korea Electrotechnology Research Institute, Chang Won 641-600, Korea.

A. V. Soukhov and G.-S. Park are with the Vacuum Electrophysics Laboratory, School of Physics, Seoul National University, Seoul 151-742, Korea.

Publisher Item Identifier 10.1109/TMTT.2002.802335.

where E_z is the longitudinal component of fundamental space harmonic amplitude of an on-axis electric field, β_0 is the propagation constant of this harmonic in the absence of an electron beam, and P is the total power flow through a interaction structure.

The measurement method commonly used for this purpose [2] employs a finite-size dielectric or conductive rod inserted into the structure as a perturber. The measurement indicates the relative electric-field strength through the change in the propagation constant of the structure. A large portion of a systematic error of the conventional perturbation theory, upon which this method is based, is attributed to the omission of the effects produced by space harmonics and TE fields [3]. The effects of the space harmonics were theoretically taken into consideration by several researchers [4], [5].

In this paper, a very thin (hairline) conductive wire is employed to minimize the effects of the space harmonics and TE fields on the interaction impedance measurement. The hairline conductive wire can be placed much closer to the helix axis where the uniform longitudinal field dominates and the effects of the space harmonics and TE fields can be fairly reduced.

This paper aims at investigating the effect of the conductive wire diameter on the measurement accuracy of the interaction impedance in order to evaluate an adequacy and limitation of such a nonresonant measurement method. The study is based on comparison of the measured data with that is obtained by a three-dimensional (3-D) finite-element numerical simulation with an automatic adaptive mesh optimization. This simulation code, i.e., HFSS [6], applies a quasi-periodic boundary condition to the helical slow-wave structure (SWS), where the phase shift per period along the axial distance is specified at the ends of the structure. The phase velocity of the helical SWS is obtained using the eigenmode solution method, where frequency versus phase shift characteristics are found by calculating the eigenfrequencies of the truncated structure satisfying the boundary condition specified. The interaction impedance of the helical SWS is obtained by directly computing E_z and P in the HFSS code.

From the nonresonant perturbation measurement, the on-axis interaction impedance for the helical SWS was derived as [7]

$$K = \frac{120}{k} \frac{\Delta\beta}{\gamma\rho} \frac{\gamma_0^2}{\beta_0^2} \frac{1}{I_0(\gamma_0\rho) \left[I_1(\gamma\rho) + \frac{I_1(\gamma\rho)}{K_0(\gamma\rho)} K_1(\gamma\rho) \right]} \quad (2)$$

where β_0 and γ_0 are the axial and radial propagation constants of the unperturbed structure, respectively. γ is the radial propagation constant of the perturbed structure and $\Delta\beta$ is the change in propagation constant between the unperturbed and perturbed structure. k is the propagation constant in free space. I_0 and K_0 are the first and second modified Bessel functions. ρ is the radius of a conductive wire. Equation (2) is derived using the nonresonant perturbation theory and scattering model of the secondary perturbed field due to the insertion of a thin conductive wire. A small perturbation is assumed to take an advantage of the very thin conductive wire. It is important that the space harmonic effect becomes negligible for a sufficiently thin conductive wire.

As shown theoretically in [7], the errors of (2) caused by other assumptions of the perturbation theory depend on the wire diameter and frequency. The accuracy verification of (2) is carried out over a 1.5-octave frequency range with a variation of a wire diameter from 2% to 30% of a helix diameter.

II. EXPERIMENT

The change in propagation constant $\Delta\beta$ and the propagation constant β_0 is measured experimentally. Fig. 1 shows the measurement

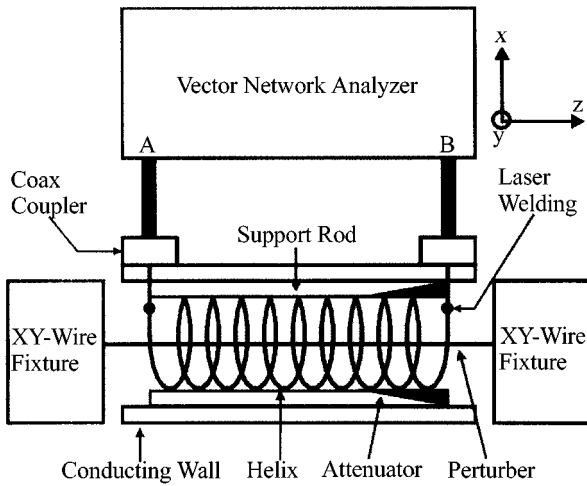


Fig. 1. Measurement setup for the interaction impedance of a helical SWS using a hairline conductive wire perturber.

setup for measuring $\Delta\beta$, which is determined by the phase change of the output signal $\Delta\Phi$ using the formula $\Delta\beta = \Delta\Phi/L$, where L is a length of the perturbed structure. As shown in Fig. 1, the helix is connected to the center conductor of a coaxial coupler by means of a laser welding so that broad-band impedance matching between the helical SWS and coupler is achieved. The S_{21} scattering parameter containing the phase information is measured before and after the conductive perturber (copper wire) is removed. To reduce reflections and end effects, a well-matched attenuator is included in the output section of the structure.

The precise positioning of the conductive wire along the axis of a helical structure is essential for an accurate measurement of interaction impedance. This is accomplished using two movable fixtures equipped with screws for the fine adjustment in transverse directions. The wire is passed through the helix and attached to the fixtures with a small tension. The fine adjustment of screws is implemented until the output phase reaches a minimum value. This minimum phase value ensures a minimum perturbation and, hence, a minimum field intensity that corresponds to the on-axis wire position. The output phase is stored in an internal memory of the vector network analyzer (VNA). The wire is then removed and the output phase is measured again to obtain $\Delta\Phi$ as a function of frequency f . The least square regression procedure is applied to the phase difference $\Delta\Phi$ versus frequency f before these values are substituted into (2).

The propagation constant β_0 in (2) is determined by the technique (similar to [8]) in which a field sensor moves along the helical structure in the axial direction and a VNA measures the phase of the traveling wave along the axis of the structure. The propagation constant $\beta_0 = d\Phi/dz$ is determined by an average slope of measured phase versus distance characteristics, where the least square regression procedure is also applied to the function $\Phi(z)$.

III. RESULTS AND DISCUSSION

The helical SWS under measurement has the following dimensions. The helix inner diameter is 1.2 mm, helix pitch is 0.65 mm, helix tape thickness is 0.1 mm, and barrel inner diameter is 3.0 mm. Three rectangular cross-sectional BeO rods with 1.5-mm width are used to support the helix. The nominal dielectric constant of BeO ($\epsilon_r = 6.5$) that was provided by the manufacturer was used for HFSS simulations. Usually, the dielectric constant of BeO is anywhere from 6 to 7.5 [9]. The structure length is approximately 80 mm.

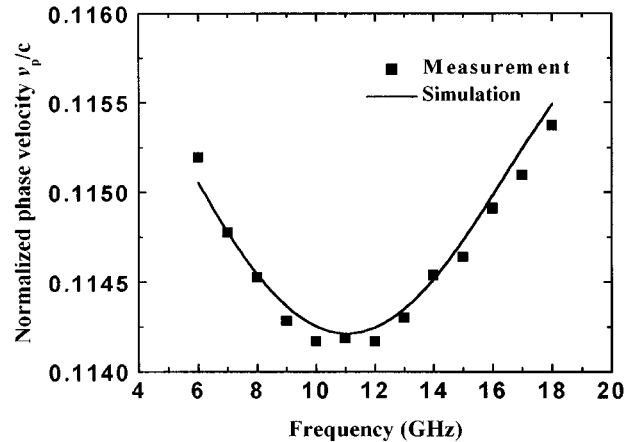


Fig. 2. Comparison of measured (by a nonresonant field sensor method) and calculated (by an HFSS code) normalized phase velocity for the helical SWS. c is the velocity of light in free space.

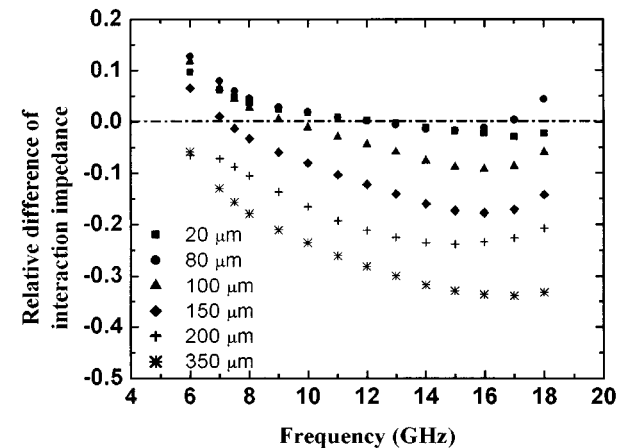


Fig. 3. Relative difference of measured and simulated interaction impedance as a function of frequency for different wire diameters.

The measured data of the phase velocity are compared with simulated results done by using the HFSS code, as shown in Fig. 2. The agreement between the calculated and measured phase velocity is better than 0.5% over the frequency range of 6–18 GHz.

The interaction impedance was measured using conductive wires with different diameters. The minimum value of $\Delta\Phi$, obtained in case of a 20- μm wire at the highest frequency of 18 GHz, was approximately 30°, which is reliably measurable with a VNA. The measurement accuracy was represented as a relative difference $(K_m - K_s)/K_s$, where K_m is the measured impedance and K_s is the simulated one. Fig. 3 demonstrates the convergence of the measured data versus wire diameter and frequency. The difference of wire diameter of 20 and 350 μm (2%–30% of the helix diameter) results in 35% change in the value of the interaction impedance, showing a significant effect of wire diameter on the interaction impedance measurement. Practically speaking, when the reference impedance values are unknown, the measurements have to be repeated several times; the perturber's size being reduced until the difference between measured data becomes less than an allowable error. The dependence of the measurement error on the frequency and the perturber's size is similar to that as predicted in [7]. It is positive at lower frequencies and negative at higher ones. As the perturber's size is reduced, the measured data converge to the reference value over the whole frequency band. Within an octave frequency range of 8–16 GHz, the interaction impedance values measured using 20- and 80- μm perturbers practically coincide with the simulated values.

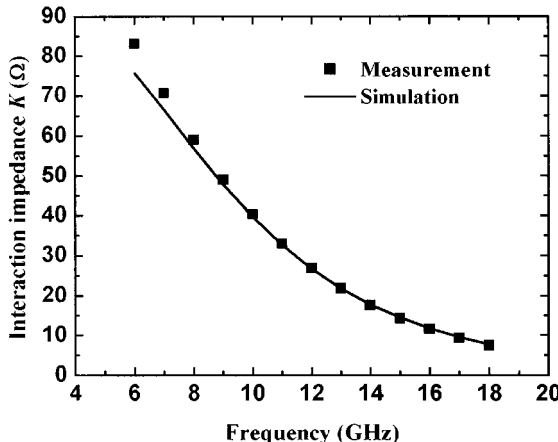


Fig. 4. Comparison of measured (by a nonresonant perturbation method using a very thin conductive wire with $20\text{-}\mu\text{m}$ diameter) and calculated (by an HFSS code) interaction impedance for the helical SWS.

The measurement with the perturber of the smallest size of $20\text{ }\mu\text{m}$ provides the best agreement with the simulation, as shown in Fig. 4. The largest discrepancy is within 10% at the lowest frequency and within 5% at the highest frequency. This discrepancy is noticeably less than that found by measurements using a dielectric perturber [3]. It seems it is the best agreement between the simulation and measurement reported for the helix interaction impedance.

IV. CONCLUSIONS

In this paper, the effects of the conductive wire on the measurement accuracy of the interaction impedance have been carried out by the nonresonant perturbation method varying the diameter of the wire. When the conductive wire diameter is approximately 2% of the helix diameter, the discrepancy between the measured and simulated values become small enough to be used for the reciprocal evaluation of software and measurement that may be helpful in TWT design. The measured values of the interaction impedance converge to the simulated ones when the wire diameter is reduced to less than 10% of the helix diameter. Therefore, the measurement method using a hairline conductive wire as a perturber is superior to the commonly used methods using a dielectric rod.

ACKNOWLEDGMENT

The authors would like to thank Dr. J. A. Dayton, Jr., Boeing and Dr. C. L. Kory for the careful reading of this paper's manuscript and for useful comments. Dr. H. S. Kim and J. H. Lee, KMW Inc., Hwa Sung City, Korea, are also acknowledged for their assistance with supplying microwave components.

REFERENCES

- [1] J. R. Pierce, *Traveling-Wave Tubes*. New York: Van Nostrand, 1950.
- [2] R. P. Lagerstrom, "Interaction impedance measurement by perturbation of traveling waves," Stanford Electron. Lab., Stanford Univ., Stanford, CA, Tech. Rep. 7, Feb. 1957.
- [3] C. L. Kory and J. A. Dayton, Jr., "Computational investigation of experimental interaction impedance obtained by perturbation for helical traveling-wave tube structures," *IEEE Trans. Electron Devices*, vol. 45, pp. 2063–2071, Sept. 1998.
- [4] P. Wang, R. Carter, and B. N. Basu, "An improved technique for measuring the Pierce impedance of helix slow-wave structures," in *Proc. Eur. Microwave Conf.*, 1994, pp. 25–30.

- [5] S. J. Rao, S. Ghosh, P. K. Jain, and B. N. Basu, "Nonresonant perturbation measurements on dispersion and interaction impedance characteristics of helical slow-wave structures," *IEEE Trans. Microwave Theory Tech.*, vol. 45, pp. 1585–1593, Sept. 1997.
- [6] *HFSS 7.0 User's Electronic Manual*, Ansoft Corporation, Pittsburgh, PA, 1999.
- [7] A. V. Soukhov, S.-S. Jung, and G.-S. Park, "Diffraction model for an interaction impedance measurement using nonresonant method," *J. Korean Phys. Soc.*, vol. 38, no. 6, pp. 762–765, June 2001.
- [8] J. R. Legarra, "Measurement of microwave characteristics of helix traveling wave circuits," in *IEEE Int. Electron Devices Meeting Tech. Dig.*, Dec. 1979, pp. 401–411.
- [9] C. L. Kory and J. A. Dayton, Jr., "Effect of helical slow-wave circuit variations on TWT cold-test characteristics," *IEEE Trans. Electron Devices*, vol. 45, pp. 972–976, Apr. 1998.

A 7.5-GHz Super Regenerative Detector

N. B. Buchanan, V. F. Fusco, and J. A. C. Stewart

Abstract—In this paper, simulated and measured results are presented for a microwave-integrated-circuit super regenerative detector operating at 7.5 GHz and brief comparisons made to a monolithic-microwave integrated-circuit super regenerative detector operating at 34 GHz. The sensitivity of the 7.5-GHz detector was measured at -83-dBm (AM, 1 kHz, 100% mod) RF signal for 12 dB (signal + noise + distortion)/(noise + distortion). Simulation results show that, to produce a sensitive super regenerative detector, a high rate of change in loop gain of the oscillator circuit with respect to the gate bias (quenching) voltage and a high maximum loop gain at the point of detection is required. It has also been shown, by simulation and measurement, that the detection frequency of the super regenerative detector is lower than the normal free-running oscillation frequency.

Index Terms—Microwave detectors, microwave oscillators, microwave receivers, super regenerative detectors.

I. INTRODUCTION

The super regenerative detector operates on the direct conversion principle where a circuit consisting of as little as one active device can perform RF detection and demodulation, allowing the possibility of a low component-count microwave receiver. In comparison, the more commonly used super heterodyne detector operates by mixing the RF signal down to a lower intermediate frequency for demodulation. This improves performance at the expense of a higher component count, which may be undesirable at millimeter-wave frequencies.

Theoretical explanations for super regenerative detectors have been described in [1]–[3] and, more recently, simulation methods have been presented in [4]. In this paper, simulated and measured results are presented for a microwave-integrated-circuit (MIC) detector operating at 7.5 GHz and brief comparisons made to a previously reported (The Queen's University of Belfast (QUB), Belfast, Northern Ireland) [5] super regenerative monolithic-microwave integrated-circuit (MMIC) detector operating at 34 GHz.

The super regenerative detector described here operates by applying a signal to the gate bias connection of an oscillator at a rate called the

Manuscript received June 11, 2001.

The authors are with the Department of Electrical and Electronic Engineering, The Queen's University of Belfast, Belfast BT9 5AH, Northern Ireland (e-mail: n.buchanan@ee.qub.ac.uk).

Publisher Item Identifier 10.1109/TMTT.2002.802336.